Dimethyl Pyrimidine Derivatives as Corrosion Inhibitors for Carbon Steel in Hydrochloric Acid Solutions

A. S. Fouda[1], Y.M. Abdallah[2] and D. Nabil[1]

Department of Chemistry, Faculty of Science, Mansoura University, Mansoura-35516, Egypt [1]
Faculty of Dentistry, Delta University for Science and Technology, Gamasa City, Egypt [2]

Abstract: The effect of some prepared compounds, namely 4,6-dimethyl pyrimidine derivatives (P-Cl), (P-NMe$_2$) and (P-OH) on the corrosion of C-steel in 1 M HCl solutions has been studied using the weight loss, potentiodynamic polarization, electrochemical frequency modulation (EFM) and electrochemical impedance spectroscopy (EIS) techniques. The results showed that the inhibition efficiency of the investigated compounds was found to depend on the concentration and the nature of the inhibitor. The efficiency of the inhibitors increases with the increase in the inhibitor concentration but decreases with a rise in temperature. Polarization results indicated that these compounds behave as mixed type inhibitors. The adsorption of these compounds on steel surface followed Langmuir adsorption isotherm. The reactivity of investigated compounds was analysed through quantum chemical by PM3 method to explain the efficiency of these inhibitors as corrosion inhibitors. The scanning electron microscope (SEM) results showed the formation of a protective film on the metal surface in the presence of these additives.

Keywords: Pyrimidine derivatives, C-steel, acid corrosion, PM3, SEM.

I. INTRODUCTION

Corrosion and corrosion inhibition of iron and iron alloys, in general, and steel, in particular, have received a great attention in different media [1– 5] with and without various types of inhibitors. The corrosion inhibition of C-steel becomes of such interest because it is widely used as a constructional material in many industries and this is due to its excellent mechanical properties and low cost. Carbon steel, the most widely used in engineering material, accounts for approximately 85 % of the annual steel production worldwide. Despite its relatively limited corrosion resistance, C-steel is used in large tonnages in marine applications, chemical processing, petroleum production and refining, construction and metal- processing equipment. The corrosion inhibition efficiency of organic compounds is related to their adsorption properties. Adsorption depends on the nature and the state of the metal surface, on the type of corrosive medium and on the chemical structure of the inhibitor [6]. Studies report that the adsorption of the organic inhibitors mainly depends on some physico-chemical properties of the molecule related to its functional group, to the possible steric effects and electronic density of donor atoms; adsorption is also supposed to depend on the possible interaction of π-orbitals of the inhibitor with d-orbitals of the surface atoms, which induce greater adsorption of the inhibitor molecules onto the surface of C-steel, leading to the formation of corrosion protecting film [7,8].

Quantum chemical calculations have been widely used to study the reaction mechanism and to interpret the experimental results as well as to solve chemical ambiguities. This is a useful approach to investigate the reaction mechanism of the inhibitors molecules and the metal surface. The structural and electronic parameters of the inhibitors molecules can be obtained by means of theoretical calculations using the computational methodologies of quantum chemistry [9].

The present work was designed to study the corrosion inhibition of C-steel in 1M HCl solutions by some pyrimidine derivatives as corrosion inhibitors using weight loss, different electrochemical techniques, also, to compare the experimental results with the theoretical ones.

In this work, we investigate the effect of some chalcone derivatives on the corrosion behavior of aluminum in 0.5 M HCl solution using chemical, electrochemical techniques and quantum chemical calculations.
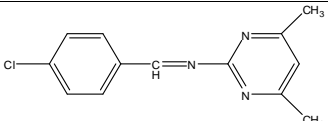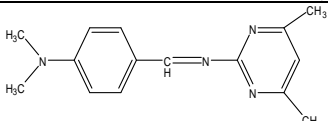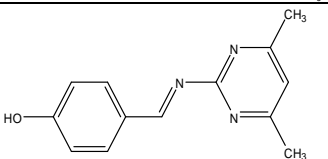
II. EXPERIMENTAL

2.1. Materials and reagents

The working electrode was mechanically cut from cylindrical carbon steel rod [having composition (weight %): C 0.2; Mn 0.9; P 0.007; Si 0.002 % and the rest Fe] of rectangular design having an area of 1 cm^2 were used in this study. The surface of working electrode was abraded using different grades (up to1200 grade) of emery papers, degreased with acetone, washed with bidistilled water and dried with soft paper. The experimental measurements were carried out in 0.1 M HCl solution in the absence and presence of various concentrations of 4,6-dimethyl **p**yrimidine derivatives for all studies. The chemical structure of 4,6-dimethyl pyrimidine derivatives is given in Table 1.These compounds were synthesized and characterized as before [10]. The concentrations of inhibitors employed were varied from 1x 10^{-6} M to 17 x 10^{-6} M. For each experiment, a freshly prepared solution was used.

Table 1: structures, molecular weights and molecular formulas of the investigated pyrimidine derivatives

	Name	Structure	Molecular weight& Chemical formula
p-Cl	4-((4,6-dimethylpyrimidin-2-ylimino)methyl) chlorobenzen. (P-Cl)		245.6 $C_{13}H_{12}N_3Cl$
p-NMe$_2$	4-((4,6-dimethylpyrimidin-2-ylimino)methyl) N,N-dimethylaniline (P-NMe$_2$)		254 $C_{15}H_{18}N_4$
p-OH	4-((4,6-dimethylpyrimidin-2-ylimino)methyl) phenol (P-OH)		227.26 $C_{13}H_{13}ON_3$

2.2. Weight loss measurements

Test pieces of C-steel (20×20×2 mm) were suspended by suitable glass hooks at the edge of the basin. The test specimen of C-steel was treated as described before and it had a total surface area of ≈8 cm^2. It was dipped in 100 ml of test solution at 25±1°C. This was conducted in a covered beaker to prevent contact with air and allow the escape of evolving gases. After the required immersion time, the test specimen was removed, washed with double distilled water, dried as before and finally weighed. The average weight loss at a certain time (180 min) for the tested samples was taken in mg cm^{-2} at the temperature of 298 K, 303 K, 308K, 313 K and 318 K in water thermostat. The change in weight was recorded to the nearest 0.0001 g. Precautions were always made to avoid scratching the specimen during washing after exposure. Therefore, the weight losses/cm^2. ΔW are given from the equations 1:

$$\Delta W = \frac{W_1 - W_2}{a} \qquad (1)$$

Where W_1 and W_2 are the weights of specimen before and after reaction, respectively and *a* is the surface area in cm^2. The inhibition or acceleration efficiency *IE* % was computed from the equation 2:

$$IE\% = \frac{\Delta W - \Delta W_i}{\Delta W} \times 100 \qquad (2)$$

Where ΔW and ΔW_i are the weight losses per unit area in the absence and presence of the investigated compounds, respectively.

2.3. Electrochemical measurements

Polarization experiments were carried out in a conventional three-electrode cell with a platinum counter electrode (1 cm^2) and a saturated calomel electrode (SCE) coupled to a fine Luggin capillary as the reference electrode. The working electrode was in the form of a square cut from c-steel embedded in epoxy resin of poly tetra fluoro ethylene (PTFE) so that the flat surface was the only surface in the electrode.

The electrochemical measurements were carried out using a Gamry instrument Potentiostat/Galvanostat/ZRA (PCI 300/4). This includes a Gamry Framework system based on the ESA400, Gamry applications that include DC105 for dc corrosion measurements, EIS300 for electrochemical impedance spectroscopy and EFM140 software for electrochemical frequency modulation measurements along with a computer for collecting data. Electrochemical data were analyzed by Echem Analyst 5.5 software. The working electrode was immersed in the test solution before starting the measurements, until a steady state was reached (30 min). For potentiodynamic polarization measurements, the potential was scanned at a scan rate of 1mVs^{-1}. Potential changed automatically from -700 mV up to +300.mV$_{SCE}$. EIS measurements were performed at open-circuit potential over a frequency range of 0.1Hz to 100 kHz. The sinusoidal potential perturbation was 5 mV in amplitude. EFM carried out using two frequencies 2.0 and 5.0 Hz. The base frequency was 1.0 Hz. We use a perturbation signal with amplitude of 10 mV for both perturbation frequencies of 2.0 and 5.0 Hz.

2.4. QUANTUM CHEMICAL STUDY

The molecular structures of the investigated compounds were optimized initially with PM3 semi empirical method so as to speed up the calculations. All the quantum chemical calculations were performed with Material studio V. 6.0.
The calculated quantum chemical parameters χ, Pi and η were calculated. The concepts of these parameters are related to each other [11-15] where:

$$P_i = -\chi \qquad (3)$$

$$P_i = \frac{(E_{HOMO} + E_{LUMO})}{2} \qquad (4)$$

$$\eta = \frac{(E_{LUMO} - E_{HOMO})}{2} = \Delta\frac{E}{2} \qquad (5)$$

The inverse of the global hardness which is designated as the softness σ:

$$\sigma = \frac{1}{\eta} \qquad (6)$$

The obtained values of χ and η were used to calculate the fraction of electrons transferred, ΔN, from the inhibitor to metallic surface [16-18] as follows:

$$\Delta N = \frac{(\chi_{steel} - \chi_{inh})}{2(\eta_{steel} + \eta_{inh})} \qquad (7)$$

where χ$_{steel}$ and χ$_{inh}$ denote the absolute electronegativity of aluminum and inhibitor molecule respectively, η$_{steel}$ and η$_{inh}$ denote the absolute hardness of aluminum and the inhibitor molecule respectively.

2.5. SCANNING ELECTRON MICROSCOPY MEASUREMENTS (SEM, EDS)

The electrode surface of C-steel was examined by Scanning Electron Microscope – type JOEL 840, Japan before and after immersion in 1 M HCl test solution in the absence and in presence of the optimum concentrations of the investigated inhibitors at 25°C, for 1 day immersion time. The specimens were washed gently with distilled water, then dried carefully and examined without any further treatments.

III. RESULTS AND DISCUSSION

3.1. Weight loss measurements

Weight loss in mg cm^{-2} of the surface area for C-steel was determined in the absence and presence of the investigated compounds. Fig. 1 shows the calculated weight loss/cm^2 for C-steel which was exposed to 1 M HCl at 25±1°C in the

absence and presence of different concentrations ranging from 1 x 10^{-6} to 17 x 10^{-6} M from compound II (P-NMe$_2$) as example for the investigated compounds. The weight loss decreased by increasing the concentration of each inhibitor at the studied temperatures 25, 30,35,40 and 45°C, so that the three investigated compounds inhibit the corrosion of C-steel in the acidic medium. Table 2 shows the inhibitor efficiency obtained (*IE* %) at the studied tested temperatures from 25 to 45°C. It is clear that the inhibition efficiency of the investigated compounds increased with increasing the inhibitor concentrations and decreased with increasing the range of temperatures. Fig. 2 shows the calculated weight loss.cm^{-2} for C-steel which is exposed to 1 M HCl at 25°Cin the absence and presence of 17 x 10^{-6} M from different investigated compounds. It is found that the percentage inhibition differs at the same concentration from one compound to another and the order of decreasing the inhibition efficiency among the investigated compounds decreases as follows: P-NMe$_2$ > P-Cl > P-OH.
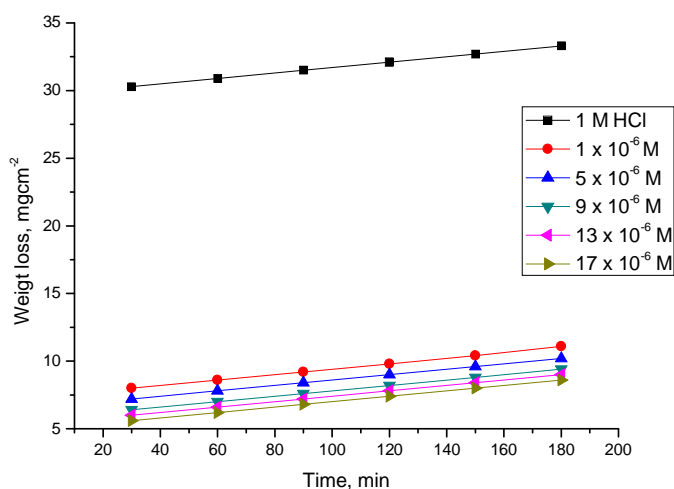

Fig. 1: Weight loss–time curves for C-steel corrosion in the presence and absence of different concentrations of p-NMe$_2$ at 25°C
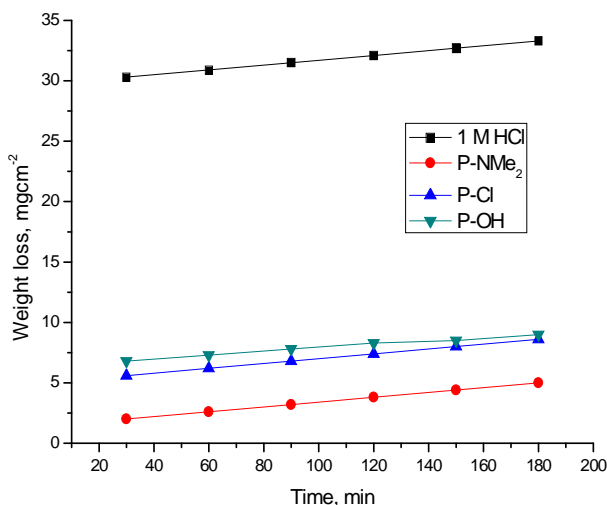

Fig. 2: Weight loss-time curve for C-steel corrosion in the presence and absence of 17 x 10^{-6} M of different compounds at 25°C

Table 2: Inhibition efficiency (IE %) of the pyrimidine derivatives at different concentrations after testing C-steel for 60 min in 1 M HCl solution at the temperature range of 25-45ºC

Inhibitor	Concentration, M	IE %				
		25ºC	30ºC	35ºC	40ºC	45ºC
p-Cl	1×10^{-6}	69.5	63.6	60.6	42.1	40
	5×10^{-6}	71.9	64.8	62.4	43.3	41.1
	9×10^{-6}	74.5	66.1	63.6	44.7	41.7
	13×10^{-6}	75.7	67.3	64.5	45.3	42.9
	17×10^{-6}	76.9	68.4	66.6	45.9	44
p-NMe$_2$	1×10^{-6}	80.1	72.7	69.9	50.9	48.6
	5×10^{-6}	82.6	73.9	70.7	52	49.7
	9×10^{-6}	85	75.2	71.9	52.6	50.3
	13×10^{-6}	86.6	76.4	73.1	53.2	51.4
	17×10^{-6}	88.2	77.6	74.3	53.8	52.8
p-OH	1×10^{-6}	63.9	57.6	54	32.2	28.5
	5×10^{-6}	66.4	58.8	54.6	33.9	29.1
	9×10^{-6}	69.2	60	55.5	35.7	31.1
	13×10^{-6}	71.7	61.2	57.6	36.8	31.7
	17×10^{-6}	74.1	62.4	58.8	37.4	32.3

3.2. POLARIZATION MEASUREMENTS

Figs. 3–5 show the polarization curves after the addition of corrosion inhibitors P-Cl, P-NMe$_2$ and P-OH. In every curve, it is observed that the current density of the anodic and cathodic branch is displaced towards lower values. This displacement is more evident with the increase in concentration of the corrosion inhibitor when compared to the blank material. The electrochemical parameters, such as current density (i_{corr}), anodic (β_a) and cathodic (β_c) slopes, were obtained by Tafel extrapolation at the corrosion potential (E_{corr}) and are listed in Table 3.It is observed that the current density decreased when the inhibitor concentration is increased and the lowest values were obtained for the P-Cl. The slopes do not display an order with the inhibitor concentration; this feature indicates that corrosion inhibitors have no effect on both hydrogen evolution and iron dissolution, it appears that inhibition occurred by a blocking mechanism on the available metal spaces [19, 20]. The corrosion potential displayed small fluctuations in the range of -523 mV around the corrosion potential of -459 mV and it tends to change towards the positive direction (Table 3). These results indicated that the presence of Pyrimidine compounds inhibited iron oxidation and in a lower extent hydrogen evolution, consequently these compounds can be classified as mixed corrosion inhibitors. The inhibition efficiency (IE %) was calculated from the polarization curves as follows:

$$IE\% = \left(1 - \frac{i_{corr}}{i^o_{corr}}\right) \times 100 \tag{8}$$

where i_{corr} and i^o_{corr} are the corrosion current densities with and without corrosion inhibitor, respectively. The corrosion inhibitor efficiency is summarized in Table 3, where it is shown that efficiency is proportional to concentration. It is important to note that there exists a difference in corrosion efficiency between weight loss tests and polarization curves, although the inhibition tendency is similar at 25ºC in both tests, probably because the former was performed for a longer time (3 h) than the latter (after reaching OCP, 0.5 h). This way ascending order of compounds as a function of inhibitor efficiency was as follows: P-NMe$_2$ > P-Cl > P-OH.

The inhibitor efficiency corroborated the importance of the molecular size and volume on the inhibition process [21, 22].

Fig.3: Potentiodynamic polarization curves for the corrosion of carbon steel in 1 M HCl in the absence and presence of different concentrations of P-Cl at 25º C

Fig. 4: Potentiodynamic polarization curves for the corrosion of carbon steel in 1 M HCl in the absence and presence of different concentrations of P-NMe$_2$ at 25º C
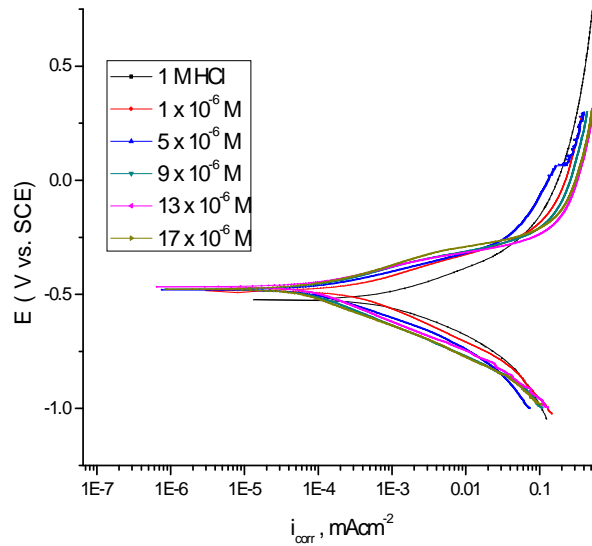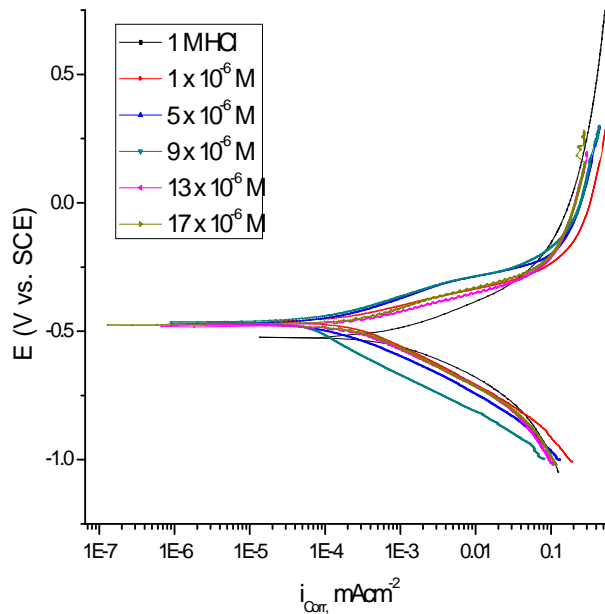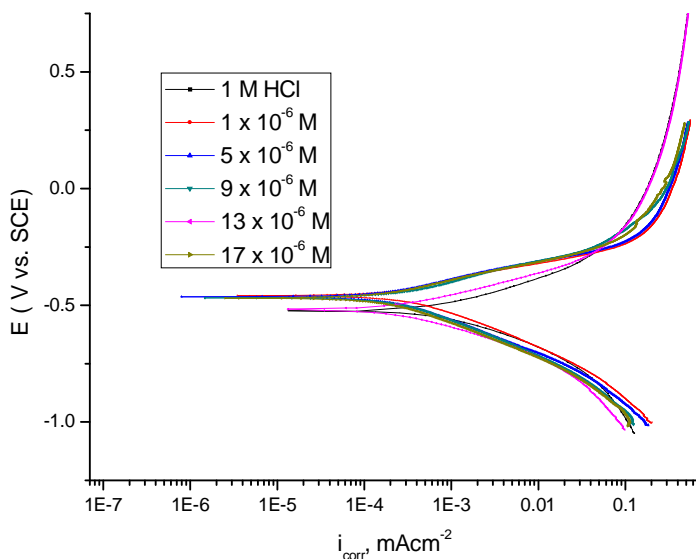
Fig. 5: Potentiodynamic polarization curves for the corrosion of carbon steel in 1 M HCl in the absence and presence of different concentrations of P-OH at 25° C

Table 3: Electrochemical parameters obtained from potentiodynamic polarization measurements of carbon steel in 1 M HCl in the absence and presence of different concentrations of investigated compounds at 25° C

Inhibitor	Conc., M	$-E_{corr}$, mV	I_{corr}, $\mu A\ cm^{-2}$	β_c, $mV\ dec^{-1}$	β_a, $mV\ dec^{-1}$	θ	$IE_{PP}\%$
p- Cl	---	523.0	981.0	169.6	149.5	---	---
	1×10^{-6}	484.0	135.0	122.5	85.70	0.862	86.2
	5×10^{-6}	480.0	99.90	127.0	80.50	0.898	89.8
	9×10^{-6}	477.0	70.10	135.6	79.30	0.929	92.9
	13×10^{-6}	467.0	68.50	131.1	72.00	0.930	93.0
	17×10^{-6}	457.0	60.30	133.3	85.10	0.939	93.9
p- NMe$_2$	---	523.0	852.0	155.0	137.6	---	---
	1×10^{-6}	479.0	99.50	130.9	95.60	0.883	88.3
	5×10^{-6}	476.0	96.00	120.6	63.50	0.887	88.7
	9×10^{-6}	464.0	54.70	159.8	79.40	0.936	93.6
	13×10^{-6}	463.0	9.20	77.90	45.80	0.989	98.9
	17×10^{-6}	460.0	8.55	77.90	48.70	0.990	99.0
p-OH	---	523.0	943.0	162.1	148.7	---	---
	1×10^{-6}	518.0	279.0	134.4	103.3	0.704	70.4
	5×10^{-6}	469.0	267.0	141.3	93.20	0.717	71.7
	9×10^{-6}	468.0	238.0	152.5	99.50	0.748	74.8
	13×10^{-6}	464.0	182.0	138.8	90.30	0.807	80.7
	17×10^{-6}	459.0	173.0	143.2	91.80	0.817	81.7

3.3. ELECTROCHEMICAL IMPEDANCE SPECTROSCOPY (EIS)

Figs. 6, 7 show the Nyquist and Bode diagrams of carbon steel in 1 M HCl solutions containing different concentrations of P-NMe$_2$ at 25°C. All the impedance spectra exhibit one single depressed semicircle. The diameter of semicircle increases with the increase of investigated inhibitor concentration. The impedance spectra exhibit one single capacitive loop, which indicates that the corrosion of steel is mainly controlled by a charge transfer process [23] and the

presence of investigated inhibitor does not change the mechanism of carbon steel dissolution [24]. In addition, these Nyquist diagrams are not perfect semicircles in 1 M HCl that can be attributed to the frequency dispersion effect as a result of the roughness and inhomogeneous of electrode surface [25]. Furthermore, the diameter of the capacitive loop in the presence of inhibitor is larger than that in the absence of inhibitor (blank solution), and increased with the inhibitor concentration. This indicates that the impedance of inhibited substrate increased with the inhibitor concentration. [24, 25]. This behavior is usually attributed to the inhomogeneity of the metal surface arising from surface roughness or interfacial phenomena [26], which is typical for solid metal electrodes [27]. Generally, when a non-ideal frequency response is presented, it is commonly accepted to employ the distributed circuit elements in the equivalent circuits. What is most widely used is the constant phase element (CPE), which has a non-integer power dependence on the frequency [28]. Thus, the equivalent circuit depicted in Figure 8 is employed to analyze the impedance spectra, where R_s represents the solution resistance, R_{ct} denotes the charge-transfer resistance, and a CPE instead of a pure capacitor represents the interfacial capacitance. The impedance of a CPE is described by the equation 9:

$$Z_{CPE} = Y_0^{-1}(j\omega)^{-n} \tag{9}$$

where Y_0 is the magnitude of the CPE, j is an imaginary number, ω is the angular frequency at which the imaginary component of the impedance reaches its maximum values, and n is the deviation parameter of the CPE: $-1 \leq n \leq 1$. The values of the interfacial capacitance C_{dl} can be calculated from CPE parameter values Y_0 and n using equation 10 [29]:

$$C_{dl} = Y_0(\omega_{max})^{n-1} \tag{10}$$

The values of the parameters such as R_s, R_{ct}, through EIS fitting as well as the derived parameters C_{dl} and IE % are listed in Table 4.
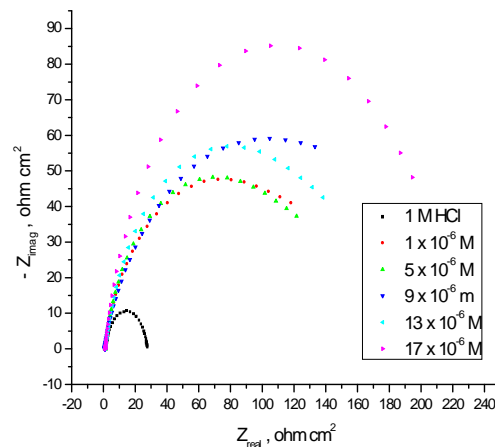

Fig. 6: Nyquist plots for corrosion of carbon steel in 1 M HCl in the absence and presence of different concentrations of p-NMe$_2$ at 25° C
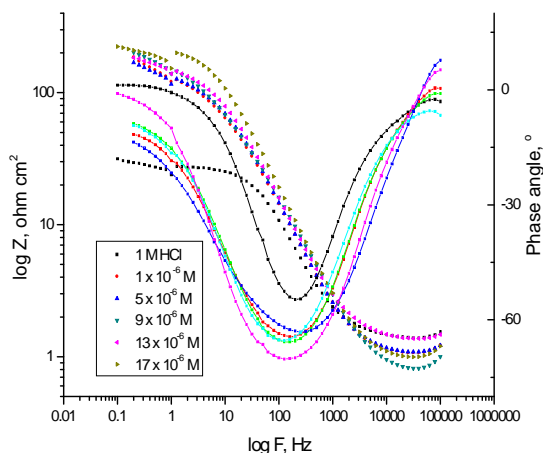
Fig. 7: Bode plots recorded for carbon steel in 1 M HCl without and with various concentrations of p-NMe$_2$ at 25˚C
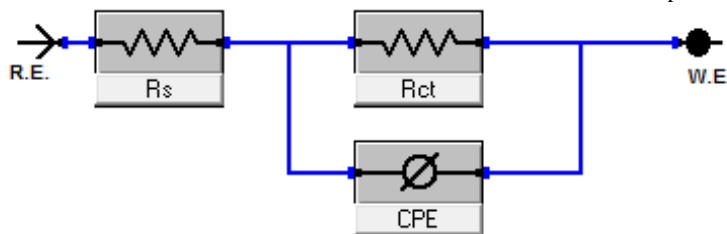

Fig. 8: Electrical equivalent circuit used to fit the impedance data

Table 4: Electrochemical kinetic parameters obtained from EIS technique for carbon steel in 1M HCl solution containing various concentrations of investigated inhibitors at 25 ˚C.

Concentration, M		R_p, kΩ cm^2	C_{dl}, μF cm^{-2}	θ	% IE
1 M HCl		24.69	1.27E-04	---	---
P-Cl	1 x 10^{-6}	97.20	1.10E-04	0.746	74.6
	5 x 10^{-6}	99.94	9.62E-05	0.753	75.3
	9 x 10^{-6}	105.10	7.19E-05	0.765	76.5
	13 x 10^{-6}	116.20	7.72E-05	0.788	78.8
	17 x 10^{-6}	156.40	6.87E-05	0.842	84.2
P-NMe$_2$	1 x 10^{-6}	106.80	1.21E-04	0.769	76.9
	5 x 10^{-6}	110.50	1.14E-04	0.777	77.7
	9 x 10^{-6}	115.60	1.09E-04	0.786	78.6
	13 x 10^{-6}	129.60	1.07E-04	0.809	80.9
	17 x 10^{-6}	180.70	8.39E-05	0.863	86.3
P-OH	1 x 10^{-6}	77.03	1.17E-04	0.679	67.9
	5 x 10^{-6}	87.90	1.16E-04	0.719	71.9
	9 x 10^{-6}	95.00	1.14E-04	0.740	74.0
	13 x 10^{-6}	99.94	9.62E-05	0.753	75.3
	17 x 10^{-6}	112.60	4.72E-05	0.781	78.1

3.4. Electrochemical frequency modulation (EFM) measurements

The EFM is a non-destructive corrosion measurement technique that can directly give values of the corrosion current without prior knowledge of Tafel constants. It is generally accepted that in most cases, the corrosion rates determined with the EFM technique, are much higher than the values determined with other techniques exhibiting low corrosion rates [30].The modulation frequencies that are used in the EFM technique are in the capacitive region of the impedance spectra. However, results of the EFM technique showed good agreement of corrosion rates obtained with the Tafel extrapolation method. Figs. 9 a-f are examples of carbon steel immersed in 1 M HCl solutions without compound (P-NMe$_2$) and others containing different concentrations of compound (P-NMe$_2$) at 25 °C. Each spectrum is a current response as a function of frequency.

The calculated corrosion kinetic parameters at different concentrations of the investigated compounds in 1 M HCl at 25 °C (i$_{corr}$, β$_a$, β$_c$, CF-2, CF-3 and % IE) are given in Table 5. From Table 5, the corrosion current densities decrease by increasing the concentration of investigated compounds and the efficiency of inhibition increases by increasing investigated compounds concentrations. The causality factors in Table 5 are very close to theoretical values, which according to EFM theory [31] should guarantee the validity of Tafel slopes and corrosion current densities. Values of causality factors in Table 5 indicate that the measured data are of good quality. The standard values for CF-2 and CF-3 are 2.0 and 3.0, respectively. The deviation of causality factors from their ideal values might be due to the perturbation amplitude which was too small or that the resolution of the frequency spectrum is not high enough. Another possible explanation is that the inhibitor is not performing very well. The obtained results showed good agreement of corrosion kinetic parameters obtained with the EFM, Tafel extrapolation and EIS methods.
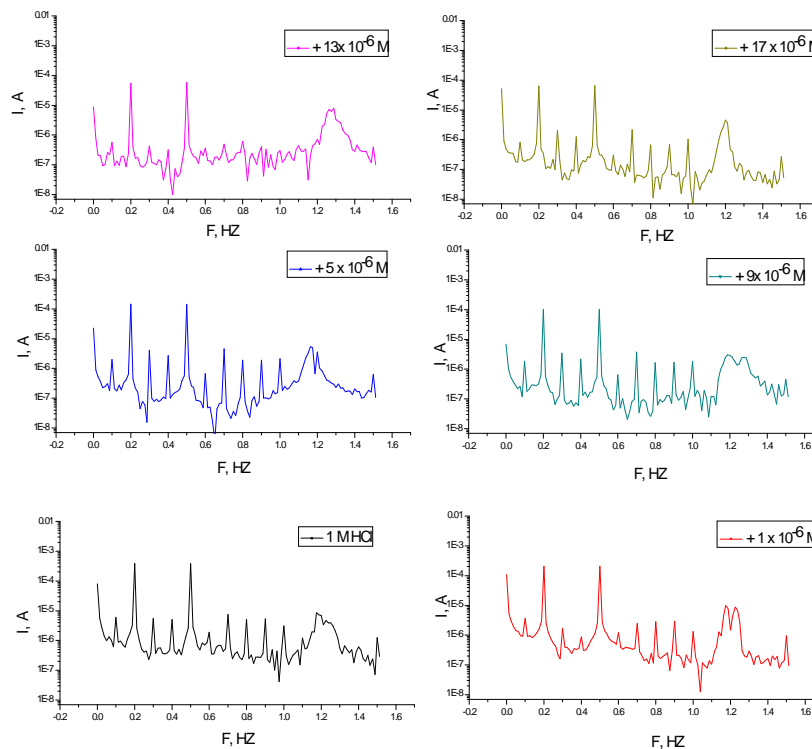

Fig. 9a- f: Intermodulation spectrum for carbon steel in 1 M HCl solutions without and with various concentrations (1x10^{-6}-17x10^{-6} M) of compound (p-NMe$_2$) at 25 °C

Table 5: Electrochemical kinetic parameters obtained by EFM technique for carbon steel in 1 M HCl solutions containing various concentrations of the investigated compounds at 25 °C

Concentration, M		i_{corr}, µA	β_a mVdec^{-1}	β_c mVdec^{-1}	C.R. mpy	CF-2	CF-3	θ	%IE
1 M HCl		551.8	89.02	98.06	252.2	1.885	2.745	---	---
p-Cl	1×10^{-6}	332.9	98.44	105.9	152.1	1.749	3.253	0.397	39.7
	5×10^{-6}	219.1	82.59	95.06	100.1	1.802	2.956	0.603	60.3
	9×10^{-6}	203.2	100.4	125.2	92.87	2.004	3.103	0.632	63.2
	13×10^{-6}	107.6	64.74	71.70	49.17	1.986	3.075	0.805	80.5
	17×10^{-6}	101.4	86.99	122.8	46.32	1.974	2.939	0.816	81.6
p-NMe$_2$	1×10^{-6}	322.7	97.49	103.7	147.5	1.874	2.853	0.415	41.5
	5×10^{-6}	200.1	83.81	99.47	91.45	1.821	3.192	0.637	63.7
	9×10^{-6}	130.9	76.23	91.43	59.80	1.833	3.080	0.763	76.3
	13×10^{-6}	100.9	111.2	117.8	46.11	1.916	2.837	0.817	81.7
	17×10^{-6}	71.56	66.89	77.16	32.70	1.846	2.905	0.870	87.0
p-OH	1×10^{-6}	294.9	95.26	99.71	134.8	1.630	2.753	0.466	46.6
	5×10^{-6}	291.6	32.29	38.11	133.2	1.761	2.823	0.472	47.2
	9×10^{-6}	278.4	94.99	100.8	127.2	2.039	2.869	0.495	49.5
	13×10^{-6}	274.5	87.40	111.3	125.4	1.884	3.226	0.503	50.3
	17×10^{-6}	210.8	92.41	96.25	96.33	2.145	3.021	0.618	61.8

3.5. EFFECT OF TEMPERATURE ON CORROSION PROCESS

The effect of temperature on both corrosion and corrosion inhibition of carbon steel in 1 M HCl solution in the absence and presence of different concentrations of investigated compounds at different temperatures ranging from 25ºC to 45ºC was studied using weight loss measurements. The corrosion rate increases with increasing temperature both in uninhibited and inhibited acid. The apparent activation energy (E^*_a) for the corrosion process can be calculated from Arrhenius-type equation [32]:

$$R_{corr} = A \exp\left(\frac{-E^*_a}{RT}\right) \tag{11}$$

where R_{corr} is the corrosion rate and A is the Arrhenius pre-exponential constant depends on the metal type and electrolyte. Plots of logarithm of the corrosion rate (log R_{corr}) with the reciprocal of absolute temperature (1/T) in the absence and presence of 17×10^{-6}M of inhibitors were shown graphically in Fig. 10. The values of (E^*_a) is summarized in Table 6. It is clear that the values of E^*_a are similar and ranging from (34.4 to 57.8 kJmol^{-1}) suggested that the inhibitors are similar in their mechanisms of action. It is also indicated that the whole process is controlled by surface reaction, since the activation energy (E^*_a) of the corrosion process is over (20 kJmol^{-1}) [33].
The enthalpy change of activation (ΔH^*) and the entropy change of activation (ΔS^*) for corrosion of carbon steel in 1 M HCl in the absence and presence of 17×10^{-6} M of each additives are calculated from the transition state theory using the following equation [34].

$$R_{corr} = \frac{RT}{Nh} \, exp\left(\frac{\Delta S^*}{R}\right) exp\left(\frac{-\Delta H^*}{RT}\right) \tag{12}$$

where h is Planck's constant, N is the Avogadro's number, ΔS^* is the entropy of activation and ΔH^* is the enthalpy of activation.

Plot of log (R_{corr}/T) vs. (1/T) for uninhibited carbon steel in 1 M HCl and in the presence of 17 x 10^{-6} M of the investigated compounds (Fig. 11) give straight lines with slope equal (-ΔH^*/2.303R) and an intercept equal (log R/Nh - ΔS^*/2.303R) from which the values of ΔH^* and ΔS^* were calculated and listed in Table 6. It is clear that the presence of tested compounds increased the activation energy values and consequently decreased the corrosion rate of the carbon steel. These results indicate that these investigated compounds acted as inhibitors through increasing activation energy of carbon steel dissolution by making a barrier by their adsorption on metal surface. The positive values of enthalpy change of activation (ΔH^*) reflect the strong adsorption of these compounds on C-steel surface and the process of the dissolution of carbon steel is endothermic process. The values of the entropy change of activation (ΔS^*) in the absence and presence of the investigated compounds are large and negative; this indicates that the activated complex in the rate-determining step represents an association rather than dissociation step. This means that the activated molecules were in higher order state than that at the initial state [35].

The order of the inhibition efficiency of the investigated compounds as gathered from the increase in E^*_a and (ΔH^*) and the decrease in (ΔS^*) values, remains unchanged and follows the order: P-NMe$_2$ > P-Cl > P-OH .

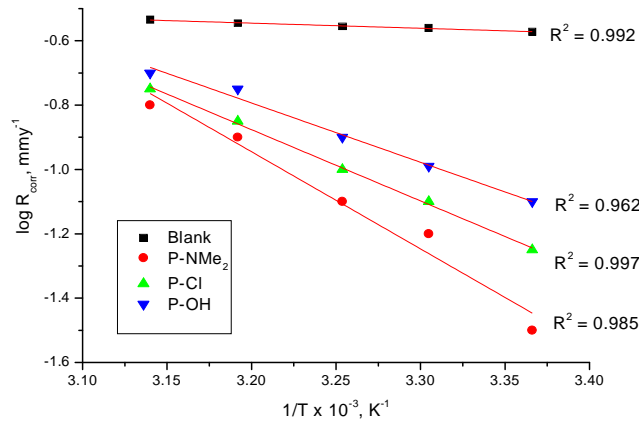Fig. 10: logarithm of the corrosion rate (log R_{corr}) with the reciprocal of absolute temperature (1/T) for carbon steel dissolution in 1 M HCl in the absence and presence of investigated inhibitors.
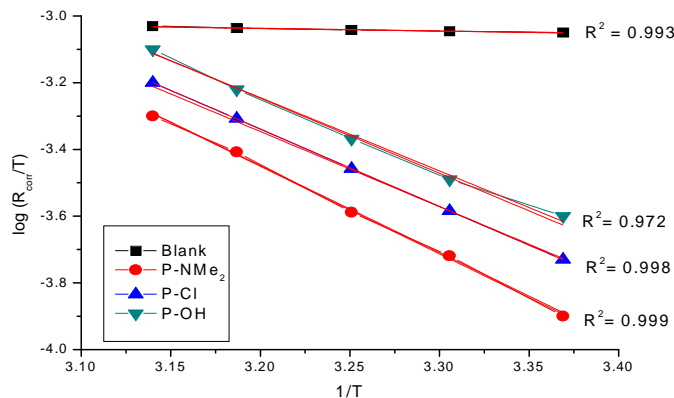

Fig. 11: log (R_{corr}/T) vs. (1/T) for uninhibited carbon steel in 1 M HCl and in the presence of investigated inhibitors.

Table 6: Activation parameters of the dissolution of carbon steel in 1 M HCl in the absence and presence of investigated compounds at 25° C

Inhibitor	Activation parameters		
	E^*_a, kJmol^{-1}	ΔH^*, kJmol^{-1}	ΔS^* J mol^{-1}K^{-1}
p-NMe$_2$	57.81	49.78	103.90
p-Cl	42.12	45.95	117.17
p-OH	34.46	42.12	122.90

3.6. ADSORPTION ISOTHERM

The mode and interaction degree between an inhibitor and a metallic surface have been widely studied with the application of adsorption isotherms. The adsorption of an organic molecule occurs because the interaction energy between an inhibitor and a metallic surface is higher than that between water molecules and a metallic surface [36, 37]. To obtain the adsorption isotherms, the degree of surface coverage (θ) was determined as a function of inhibitor concentration. The values of θ were then plotted to fit the most suitable model of adsorption [38]. Fig. 12 show the dependency of the relationship C_{inh} /θ as a function of the corrosion inhibitor concentration (C_{inh}) for investigated inhibitors. Graph yielded a good fitting with a correlation factor of unity, which suggests that the compounds under study displayed an adsorption isotherm of the Langmuir type:

$$\frac{C_{inh}}{\theta} = \frac{1}{K_{ads}} + C_{inh} \tag{13}$$

$$K_{ads} = \frac{1}{55.5} \exp\left(\frac{-\Delta G^\cdot_{ads}}{RT}\right) \tag{14}$$

where C_{inh} is the inhibitor concentration in the total volume of the test solution, and K_{ads} is the equilibrium adsorption constant involved in chemical reaction. Several authors have correlated the Langmuir isotherm with the interaction of adsorbed species on metallic surface [39,40]. The tendency of data indicates that inhibitor molecules are adsorbed on the metallic surface to form a film that isolates metal from the corrosive environment. The values of K_{ads} decreased as temperature increased (Table 7), which indicates the presence of a rearrangement and detachment of the corrosion inhibitor molecules from the metallic surface with a consequent decay in inhibitor efficiency.
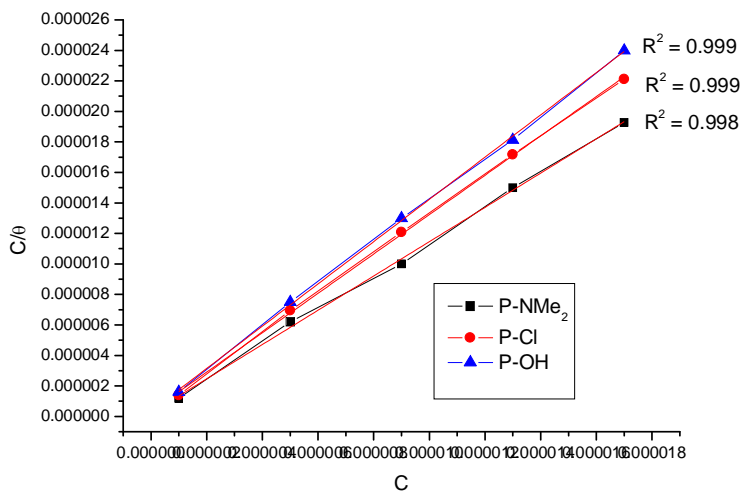

Fig. 12: C_{inh}/θ vs. C_{inh} to fitting of Langmuir's isotherm for carbon steel in 1 M HCl to determine the thermodynamic parameters of investigated inhibitors at 25°C

Table 7: Thermodynamic parameters for investigated compounds as corrosion inhibitors of carbon steel in 1 M HCl as a function of temperature.

Inhibitor	Temperature, K	R^2	K_{ads} x 10^5 M^{-1}	$-\Delta G^o_{ads}$ (kJ mol^{-1})
P-Cl	298	0.981	30.303	20.21
	303	0.999	24.691	20.481
	308	0.968	21.978	20.69
	313	0.960	20.00	20.9
	318	0.984	14.492	20.99
p- NMe$_2$	298	0.996	45.454	20.8
	303	0.996	38.461	20.95
	308	0.984	28.571	20.97
	313	0.979	23.584	21.10
	318	0.971	19.607	21.23
p-OH	298	0.996	26.315	20.2
	303	0.998	24.183	20.25
	308	0.974	18.181	20.3
	313	0.957	12.820	20.43
	318	0.981	10.869	20.5

3.7. SEM- EDX INVESTIGATION

SEM and EDX experiments were carried out in order to verify if the investigated compounds are in fact adsorbed on C-steel surface or just pealed off the surface. SEM images were indicative of the changes that accompany both corrosion and protection of the carbon steel surface (Fig. 13a–e). Figure 13a shows the free metal. Figure 13b shows the damage caused to the surface by hydrochloric acid. Figure 13c, d, e shows SEM images of the carbon steel surface after treatment with 1 M HCl containing 17 x 10^{-6} M of investigated inhibitors. From these images, it is obvious that the steel surface seems to be almost unaffected by corrosion. This is because of adsorption of investigated inhibitors forming a thin protective film of the inhibitors on the metal surface. This film is responsible for the highly efficient inhibition by these inhibitors.

The corresponding EDS profile analyses are presented in Table 8 and Figure 14 for investigated compounds not shown. It is also important to notice the existence of C and N peaks in the EDS spectra of the C-steel surface corresponding to the samples immersed for 1 day in solutions containing the optimum concentration of these compounds. The formation of a thin inhibitor film is in agreement with the SEM observations.
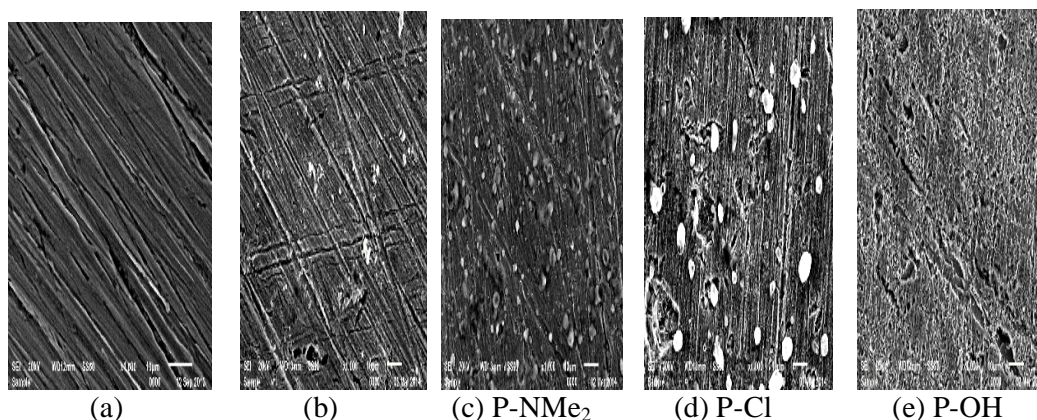

(a)   (b)   (c) P-NMe$_2$ (d) P-Cl   (e) P-OH

Fig. 13: SEM micrograph of carbon steel free (a), after immersion for 24 h in 1 M HCl alone (b) or containing 17 x 10^{-6} M of investigated inhibitors (c, d, and e).
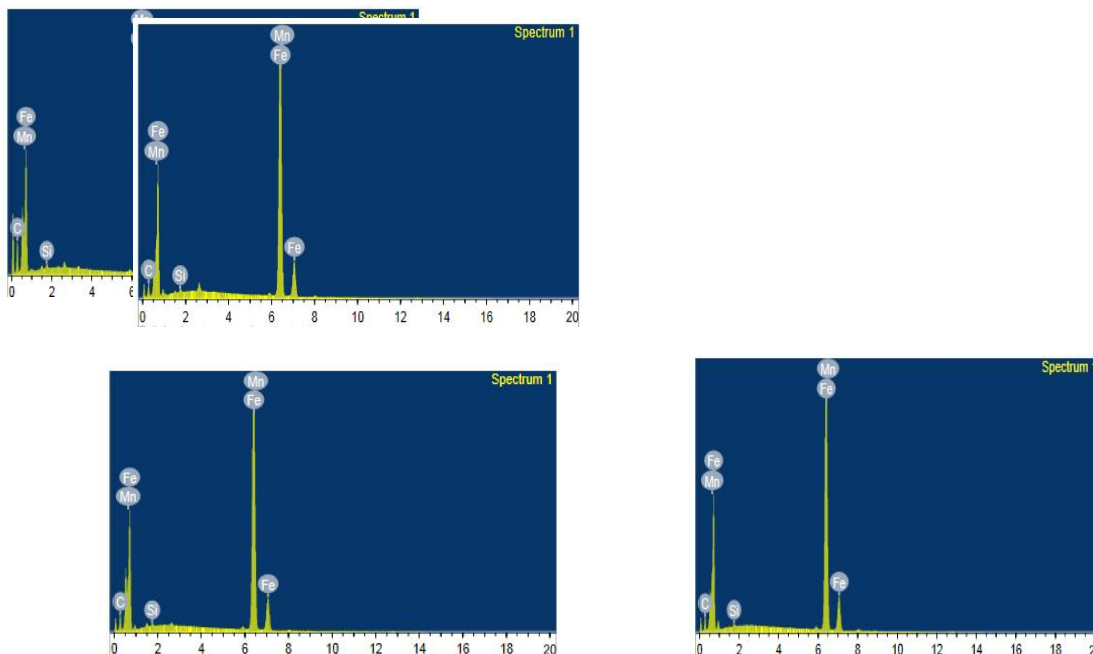
Fig. 14: EDS spectra of C-steel in 1 M HCl (a), , in the presence of 17 x 10^{-6}M p-NMe$_2$ (b) , in 17 x 10^{-6}M p-Cl (c) and in 17 x 10^{-6}M of p-OH (d)

Table 8: Surface composition (wt %) of c-steel after 1 day of immersion in 1 M HCl + 17 x 10^{-6} M of investigated inhibitors

Mass %	C	Si	Mn	Fe
Blank	37.19	0.49	0.49	61.83
P-NMe$_2$	56.60	0.47	0.30	42.62
P-Cl	42.48	0.47	0.50	56.56
P-OH	37.93	0.38	0.54	61.16

3.8. QUANTUM CHEMICAL STUDY

The E$_{HOMO}$ indicates the ability of the molecule to donate electrons to an appropriated acceptor with empty molecular orbitals, whereas the E$_{LUMO}$ indicates its ability to accept electrons. The lower value of E$_{LUMO}$, the more ability of the molecule to accept electrons [41]. The PM3 calculations showed a correlation between the molecular area of the molecule and the inhibition efficiency. The inhibition efficiency increases as the molecular area of the molecule increases due to the increase of the contact area the molecule and surface of the metal. The use of optimization analysis to estimate the adsorption centers of inhibitors has been widely reported and it is mostly used for the calculation of the charge distribution over the whole skeleton of the molecule [42].
There is a consensus by several authors that the more negatively charged hetero atom is, the more is its ability to adsorb on the metal surface through a donor–acceptor type reaction [43-45].Variation in the inhibition efficiency of the inhibitors depends on the presence of electronegative O- and N- atoms as substituent in their molecular structure. The optimized structures of inhibitors are presented in Fig. 15.
In a corrosion system, the inhibitor acts as a Lewis base while the metal acts as a Lewis acid. Bulk metals are soft acids and thus soft base inhibitors are most effective for acidic corrosion of those metals. Accordingly, it is concluded that inhibitor with the highest σ value has the highest inhibition efficiency Table 9 which is in a good agreement with the

experimental data. This also confirmed from the calculated inhibition efficiencies of molecules as a function of the inhibitor chemical potential, P_i and the fraction of the charge transfer, ΔN to metal surface. The relatively good agreement of P_i and ΔN with the inhibition efficiency could be related the fact that factor causing an increase in P_i and ΔN would enhance the electronic releasing power of the inhibitor molecule (Table 9).

Fig. 15: The optimized molecular structures, HOMO, LUMO and optimaization structures of the protonated inhibitors molecules using PM3 method.
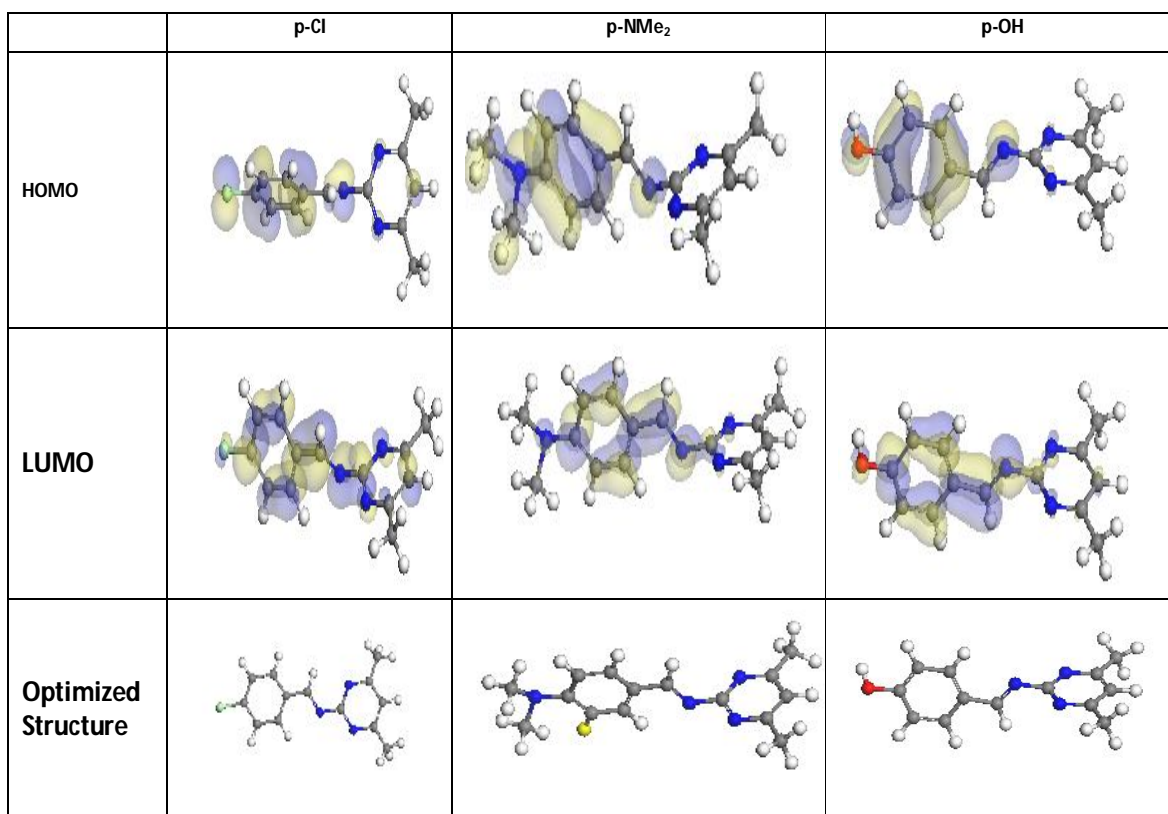

Table 9: The calculated quantum chemical parameters for protonated compounds

	Parameter	P-Cl	P-NMe$_2$	P-OH
	E_{HOMO} (eV)	-9.594	-8.914	-9.411
	E_{LUMO} (eV)	-0.96	-0.842	-0.778
	ΔE (eV)	8.634	8.072	8.633
	μ (debyes)	4.503	2.883	2.485
	η (eV)	4.317	4.036	4.317
PM3	σ (eV^{-1})	0.232	0.248	0.231
	P_i (eV)	-5.277	-4.878	-5.095
	χ (eV)	5.277	4.878	5.095
	ΔN (e)	0.611	0.604	0.590
	Molecular area (Å^2)	271.435	308.118	266.198

3.9. MECHANISM OF CORROSION

The adsorption of investigated compounds can be attributed to the presence of polar unit having atoms of nitrogen, sulphur and oxygen and aromatic/heterocyclic rings. Therefore, the possible reaction centers are unshared electron pair of hetero-atoms and л-electrons of aromatic ring [46]. The adsorption and inhibition effect of 4, 6-dimethyl Pyrimidine derivatives in 1 M HCl solution can be explained as follows: In general, two modes of adsorption are considered on the metal surface in acid media. In the first mode, the neutral molecules may be adsorbed on the surface of metal through the chemisorption mechanism, involving the displacement of water molecules from the carbon steel surface and the sharing electrons between the hetero- atoms and C-steel. The inhibitor molecules can also adsorb on the metal surface. In the second mode, since it is well known that the C-steel surface bears positive charge in acid solution [45], so it is difficult for the protonated molecules to approach the positively charged metal surface due to the electrostatic repulsion. Since chloride ions have a smaller degree of hydration, thus they could bring excess negative charges in the vicinity of the interface and favor more adsorption of the positively charged inhibitors molecules, the protonated inhibitors adsorb through electrostatic interactions between the positively charged molecules and the negatively charged metal surface. Thus there is a synergism between adsorbed Cl^- ions and protonated inhibitors. Thus we can conclude that inhibition of C-steel corrosion in 1 M HCl is mainly due to electrostatic interaction. The decrease in inhibition efficiency with rise in temperature supports electrostatic interaction.

IV. CONCLUSIONS

From the overall experimental results the following conclusions can be deduced:

1. The investigated compounds are good inhibitors and act as mixed type inhibitors for C-steel corrosion in 1 M HCl solution.

2. The results obtained from all electrochemical measurements showed that the inhibiting action increases with the inhibitor concentration and decreases with the increasing in temperature.

3. Double layer capacitances decrease with respect to blank solution when the inhibitor is added. This fact confirms the adsorption of these molecules on the carbon steel surface.

4. The adsorption of inhibitor on C-steel surface in HCl solution follows Langmuir isotherm for these compounds.

5. The values of inhibition efficiencies obtained from the different independent quantitative techniques used show the validity of the results.

6. Quantum chemical parameters for these investigated compounds were calculated to provide further insight into the mechanism of inhibition of the corrosion process.

REFERENCES

[1] W. Huilong, Z. Jiashen, L. Jing, "Inhibition of the corrosion of carbon steel in hydrochloric acid solution by bisquaternary ammonium salt", Anti-Corros. Methods and Mater. vol. 49, pp.127-132, 2002.

[2] M. T. Said, S. A. Ali, S. U. Rahman, " The cyclic hydroxyl amines: a new class of corrosion inhibitors of carbon steel in acidic medium", Anti-Corros. Methods and Materials, vol. 50, pp.201-207, 2003.

[3] A. Atia, M. M. Saleh, "Inhibition of acid corrosion of steel using cetylpyridinium chloride", J. Appl. Electrochem., vol. 33, pp. 171- 177, 2003.

[4] S. Tamilselvi, S. Rajeswari, "The effect of triazoles and surfactants on the corrosion inhibition of carbon steel in acid solution", Anti-Corros. Methods and Materials, vol. 50, pp. 223-231, 2003.

[5] S. T. Keera, "The beneficial influence of halide ions on the inhibition characteristics of nitrogen-containing organic inhibitors to reduce the corrosion rate of carbon steel in HCl", Anti-Corros. Methods and Materials, vol. 50, pp. 280-285, 2003.

[6] F. Bentiss, M. Lagrenée, M. Traisnel, J. C. Hornez, "The corrosion inhibition of mild steel in acidic media by a new triazole derivative", J. Corros. Sci., vol. 41, pp. 789-803, 1999.

[7] F. Bentiss, M. Lagrenée, M. Traisnel, " 2,5-bis(n-pyridyl)-1 3,4-oxadiazoles as corrosion inhibitors for mild steel in acidic media", J. Corros.,vol. 56, pp. 733-742, 2000.

[8] F. Bentiss, M. Traisnel, M. Lagrenée, " Influence of 2,5-bis(4-dimethylaminophenyl)-1,3,4-thiadiazole on corrosion inhibition of mild steel in acidic media", J. Appl. Electrochem., vol. 31, pp. 41-48, 2001.

[9] F. B. Growcock, V. R. Lopp, "The inhibition of steel corrosion in hydrochloric acid with 3- phenyl-2-propyn-1-ol", corros. Sci., vol. 28, pp. 397-410, 1988.

[10] A.S. Fouda, A. F. Hassan, M. A. Elmorsi, T. A. Fayed, A. Abdelhakim, "Chalcones as environmentally- friendly corrosion inhibitors for stainless steel type 304 in 1 M HCl solutions" Int. J. Electrochem. Sci., vol. 9, pp. 1298- 1320, 2014.

[11] P. Geerlings, F. De Proft, W. Langenaeker, "Conceptual density functional theory", Chem. Rev., vol. 103, pp. 1793- 1873, 2003.

[12] V. S. Sastri, J. R. Perumareddi, "Molecular Orbital Theoretical Studies of Some Organic Corrosion Inhibitors", Corrosion, vol. 53, 617-622, 1997.

[13] I. Lukovits, E. Kalman, F. Zucchi, " Corrosion Inhibitors—Correlation between Electronic Structure and Efficiency", Corrosion, vol. 57, pp. 3-8, 2001.

[14] S. Martınez, "Inhibitory mechanism of mimosa tannin using molecular modeling and substitutional adsorption isotherms", Mater. Chem. Phys., Vol. 77, pp. 97-102, 2003.

[15] F. Bentiss, C. Jama, B. Mernari, H. ElAttari, L. ElKadi, M. Lebrini, M. Traisnel, M. Lagrenee, " Corrosion control of mild steel using 3,5-bis(4-methoxyphenyl)-4-amino-1,2,4-triazole in normal hydrochloric acid medium", Corros.Sci., Vol. 51, PP.1628-1635, 2009.

[16] M. Benabdellah, A. aouniti, A. Dafali, B. Hammouti, M. Benkaddour, A. Yahyi, A. Ettouhami, A., "Investigation of the inhibitive effect of triphenyltin 2-thiophene carboxylate on corrosion of steel in 2 M H_3PO_4 solutions", Appl. Surf. Sci., vol. 252, pp. 8341-8347, 2006.

[17] A. A. Aksut, W. J. L.Lorenz, F. Mansfeld, " The determination of corrosion rates by electrochemical d.c. and a.c. methods — II. Systems with discontinuous steady state polarization behavior", Corros.Sci., vol. 22, pp. 611-619, 1982.

[18] W. J. Lorenz, F. Mansfeld, "Determination of corrosion rates by electrochemical DC and AC methods", Corros. Sci., vol. 21, pp. 647-672, 1981

[19] K. C. Emeregül, M. Hayval," Studies on the effect of a newly synthesized Schiff base compound from phenazone and vanillin on the corrosion of steel in 2 M HCl", Corros. Sci., vol. 48, pp. 797–812, 2006.

[20] A. K. Satapathy, G. Gunasekaran, S.C. Sahoo, K. Amit, P. V. Rodrigues, "Corrosion inhibition by Justicia gendarussa plant extract in hydrochloric acid solution", Corros. Sci., vol. 51, pp. 2848–2856, 2009.

[21] M. G. Hosseini, H. Khalilpur, S. Ershad, "Protection of mild steel corrosion with new thia-derivative Salens in 0.5 M H_2SO_4 solution", J. Appl. Electrochem., vol. 40, pp. 215–223, 2010.

[22] M. Elayyachy, M. Elkodadi, A. Aouniti, A. Ramdani, B. Hammouti, F. Malek, A. Elidrissi, "New bipyrazole derivatives as corrosion inhibitors for steel in hydrochloric acid solutions", Mater. Chem. Phys., vol. 93, pp. 281–285, 2005.

[23] M. Behpour, S. M. Ghoreishi, N. Mohammadi, N. Soltani, M. Salavati-Niasari, " Investigation of some Schiff base compounds containing disulfide bond as HCl corrosion inhibitors for mild steel ", Corros. Sci., vol.52, pp. 4046- 4057, 2010.

[24] L. Larabi, Y. Harek, M. Traianel, A. Mansri, " Synergistic Influence of Poly(4-Vinylpyridine) and Potassium Iodide on Inhibition of Corrosion of Mild Steel in 1M HCl ", J. Appl. Electrochem., vol. 34, pp. 833- 839, 2004.

[25] M. Lebrini, M. Lagrenee, H. Vezin, M. Traisnel, F. Bentiss, " Experimental and theoretical study for corrosion inhibition of mild steel in normal hydrochloric acid solution by some new macrocyclic polyether compounds", Corros. Sci., vol. 49, pp. 2254- 2257, 2007.

[26] S. Martinez, M. Metikoš-Hukovic, "A nonlinear kinetic model introduced for the corrosion inhibitive properties of some organic inhibitors ", J. Appl. Electrochem., vol. 33, pp. 1137- 1142, 2003.

[27] M. N. El-Haddad, A. S. Fouda, " CORROSION INHIBITION AND ADSORPTION BEHAVIOR OF SOME AZO DYE DERIVATIVES ON CARBON STEEL IN ACIDIC MEDIUM: SYNERGISTIC EFFECT OF HALIDE IONS", Chem. Eng. Comm., vol. 200, pp. 1366- 1393, 2013.

[28] J. L. Trinstancho-Reyes, M. Sanchez-Carrillo, R. Sandoval-Jabalera, V. M. Orozco-Carmona, F. Almeraya-Calderon, J. G. Chacon-Nava, J. G. Gonzalez-Rodriguez, Martínez-Villafane," Electrochemical Impedance Spectroscopy Investigation of Alloy Inconel 718 in Molten Salts at High Temperature", Int. J. Electrochem. Sci., vol. 6, pp. 419-431, 2011.

[29] C. S. Hsu, F. Mansfeld, "Concerning the Conversion of the Constant Phase Element Parameter Y_0 into a Capacitance ", Corrosion, vol. 57, pp. 747-748, 2001.

[30] E. Kus, F. Mansfeld, "An evaluation of the electrochemical frequency modulation (EFM) technique ", Corros. Sci., vol. 48, pp. 965- 979, 2006.

[31] R. K. Dinnappa, S. M. Mayanna, "Benzoic acid and substituted benzoic acids as interfacial corrosion inhibitors for copper in HClO4 ", J. Appl. Elcreochem., vol. 11, pp. 111- 116, 1982.

[32] K. Allam, Nageh, "Thermodynamic and quantum chemistry characterization of the adsorption of triazole derivatives during Muntz corrosion in acidic and neutral solutions ", Appl. Surf. Sci., vol.253, pp. 44570- 4577, 2007.

[33] K. K. Al-Neami, A. K. Mohamed, I. M. Kenawy, A. S. Fouda, "Inhibition of the corrosion of iron by oxygen and nitrogen containing compounds", Monatsh. Chem., vol. 126, pp. 369- 376, 1995.

[34] S. Martinez, I. Stern, "Thermodynamic characterization of metal dissolution and inhibitor adsorption processes in the low carbon steel/mimosa tannin/sulfuric acid system ", Appl. Surf. Sci., vol. 199, pp. 83- 99, 2002.

[35] S. S. Abd El-Rehim, M. A. M. Ibrahim, K. F. Khaled, " 4-Aminoantipyrine as an inhibitor of mild steel corrosion in HCl solution", J. Appl. Electrochem., vol. 29, pp. 593- 599, 1999.

[36] J. O. Bockris, D. A. J. Swinkels, "Adsorption of normal decylamine on solid metal electrodes", J. Electrochem. Soc., vol. 111, pp. 736–743, 1964.

[37] M. M. Saleh, A. A. Atia, "Effects of structure of the ionic head of cationic surfactant on its inhibition of acid corrosion of mild steel", J. Appl. Electrochem., vol. 36, pp. 899–905, 2006.

[38] L. Narvaez, E. Cano, D. M. Bastidas, "3-Hydroxybenzoic acid as AISI 316L stainless steel corrosion inhibitor in a H2SO4-HF-H2O2 pickling solution", J. Appl. Electrochem., vol. 35 pp. 499–506, 2005.

[39] E. Bayol, K. Kayakirilmaz, M. Erbil, "The inhibitive effect of hexamethylenetetramine on the acid corrosion of steel", Mater. Chem. Phys., vol. 104, pp. 74–82, 2007.

[40] L. Tang, G. Mu, G. Liu, "The effect of neutral red on the corrosion inhibition of cold rolled steel in 1.0 M hydrochloric acid", Corros. Sci., vol. 45, pp.2251–2262, 2003.

[41] G. Gao, C. Liang, "Electrochemical and DFT studies of β-amino-alcohols as corrosion inhibitors for brass", Electrochim. Acta, vol. 52, pp. 4554- 4559, 2007.

[42] F. Kandemirli, S. Sagdinc, "Theoretical study of corrosion inhibition of amides and thiosemicarbazones", Corros. Sci., vol. 49, pp. 2118–2130, 2007.

[43] G. Bereket, C. Ogretic, C. Ozsahim, "Quantum chemical studies on the inhibition efficiencies of some piperazine derivatives for the corrosion of steel in acidic medium", J. Mol. Struct. (THEOCHEM), vol. 663, pp. 39- 46, 2003.

[44] W. Li, Q. He, C. Pei, B. Hou, " Experimental and theoretical investigation of the adsorption behaviour of new triazole derivatives as inhibitors for mild steel corrosion in acid media", Electrochim. Acta, vol. 52, pp. 6386- 6394, 2007.

[45] B. Jiang, M. Kunimoto, M. Yanagisawa, T. Homma, "Effect of Thiourea on Oxidation of Hypophosphite Ions on Ni Surface Investigated by Raman Spectroscopy and DFT Calculation Electrochemical/Electroless Deposition",J. Electrochem. Soc., vol. 160, pp. 366- 371, 2013.

[46] Y. C. Wu, P. Zhang, H. W. Pickering, D. L. Allara, "Effect of KI on Improving Copper Corrosion Inhibition Efficiency of Benzotriazole in Sulfuric Acid Electrolytes", J.Electrochem.Soc., vol. 140, pp. 2791-2800, 1993.